Approximate dynamical eigenmodes of the Ising model with local spin-exchange moves

Wei Zhong,* Debabrata Panja, and Gerard T. Barkema
Department of Information and Computing Sciences, Utrecht University, Princetonplein 5, 3584 CC Utrecht, the Netherlands

(Received 5 March 2019; revised manuscript received 4 July 2019; published 23 July 2019)

We establish that the Fourier modes of the magnetization serve as the dynamical eigenmodes for the two-dimensional Ising model at the critical temperature with local spin-exchange moves, i.e., Kawasaki dynamics. We obtain the dynamical scaling properties for these modes and use them to calculate the time evolution of two dynamical quantities for the system, namely, the autocorrelation function and the mean-square deviation of the line magnetizations. At intermediate times $1 \lesssim t \lesssim L^{z_c}$, where $z_c = 4 - \eta = 15/4$ is the dynamical critical exponent of the model, we find that the line magnetization undergoes anomalous diffusion. Following our recent work on anomalous diffusion in spin models, we demonstrate that the generalized Langevin equation with a memory kernel consistently describes the anomalous diffusion, verifying the corresponding fluctuation-dissipation theorem with the calculation of the force autocorrelation function.

DOI: 10.1103/PhysRevE.100.012132

I. INTRODUCTION

For physical systems in statistical physics, the eigenvalues and eigenvectors (of the Hamiltonians) play a central role. The eigenvectors form a complete orthogonal basis in the space of variables used to express the Hamiltonian. The eigenvalues and eigenfunctions identify the ground and the excited states, as well as their energies, which then form the groundwork for obtaining the partition function, the principal quantity of interest for calculating all equilibrium ensemble-averaged observables.

For classical systems, the Hamiltonian also dictates the dynamics of systems through the equations of motion. Here too, theoretically, the same concept holds, *viz.,* with the equation of motion of a degree of freedom q used to describe a Hamiltonian $\mathcal{H}$ being given by

$$\zeta \dot{q} = -\frac{\partial \mathcal{H}}{\partial q}, \tag{1}$$

with ζ being the friction coefficient in the overdamped limit, it really is an asset to know the *dynamical* eigenvalues and eigenvectors. Together, the dynamical eigenvalues and eigenvectors ensure that the full time dependence of any dynamical quantity can be calculated exactly.

In contrast to eigenvalues and eigenvectors of the Hamiltonian itself, the scope for dynamical eigenvalues and eigenvectors is far more restricted, for the following reason. The eigenvectors $\{r_\alpha\}$ are linear combinations of all the degrees of freedom $\{q_i\}$, reducing Eq. (1) to the form

$$\zeta_\alpha \dot{r}_\alpha = -\lambda_\alpha r_\alpha, \tag{2}$$

with λ_α being the corresponding *dynamical* eigenvalue, obtained from the diagonalization of the Hessian matrix $\frac{\partial^2 \mathcal{H}}{\partial r_\beta \partial r_\gamma}$. The dynamical eigenmodes $\{r_\alpha\}$, if they exist, are often simply called the *modes* of the system. For the form (2) to hold, the Hessian must be independent of $\{r_\alpha\}$, which restricts the class of such Hamiltonians only to harmonic ones (i.e., $\mathcal{H}$ is quadratic in $\{q_i\}$). Classic examples of such systems are the bead-spring models of linear polymeric systems [1,2], their extensions to star and tadpole polymers [3], polymeric membranes [4,5], 2D cytoskeleton of cells [6–8], and graphite oxide sheets [8–11].

Not all is lost, however, if the Hamiltonian is not harmonic (which is in fact almost always the case). Note here that *any* complete orthogonal basis in the space of the degrees of freedom can be used to describe the dynamics of the system. The main disadvantage of choosing an arbitrary one is that the corresponding amplitudes remain dynamically (nonlinearly) coupled at all times, preventing one from taking large time steps in computer simulations. Despite this shortcoming, sometimes one can be lucky to realize that there are *approximate* modes that can allow one to take somewhat large time steps within a preordained error margin. Examples are the Rouse modes for self-avoiding polymers [12], a reptating polymer chain [13], and polymer chains in a melt [14–16].

The focus of the present paper is the (approximate dynamical) modes of the two-dimensional (2D) square-lattice Ising model (system size $L \times L$) with local spin exchange moves—commonly known as Kawasaki moves [17]—at critical temperature and at zero order parameter, introduced in Sec. II A. We focus on the line magnetization for this model and find, surprisingly, that the Fourier modes provide a very good approximation of the true dynamical eigenmodes. We numerically investigate the properties of these modes in Sec. II B–II D, numerically revealing that the equilibrium amplitude of the pth mode behaves as $(L/p)^{\gamma/\nu}$ $(B_0 + B_1 p^{-\gamma/\nu})$, and that its decay time scales $\sim (L/p)^{z_c}$, where $\gamma = 7/4$, $\nu = 1$, and $\eta = 2 - \gamma/\nu = 1/4$ are the three equilibrium critical exponents of the Ising model, and $z_c = 4 - \eta = 15/4$ is the critical dynamical exponent for the model with local spin exchange moves [18–20]. In Sec. III we use these results to analytically calculate two observables: the autocorrelation function and the mean-square deviation

*w.zhong1@uu.nl

(MSD) of the line magnetization. We find that line magnetization exhibits anomalous diffusion. Our results for anomalous diffusion is consistent with a pattern that the dynamics of magnetization at the critical temperature in spin models is anomalous [21–23]. Importantly, the anomalous diffusion is described by the generalized Langevin equation (GLE) [22,23] (and bears strong resemblance to anomalous diffusion in polymeric and membrane systems under a variety of circumstances [3,5,12,24–37]), which we verify in Sec. IV. We conclude the paper in Sec. V.

II. THE MODEL AND THE FOURIER MODES AS THE APPROXIMATE DYNAMICAL MODES

A. Ising model with local spin-exchange (Kawasaki) dynamics

We consider the 2D Ising model on an $L \times L$ square lattice with periodic boundary conditions in both x and y directions. The Hamiltonian for the model is given by

$$\mathcal{H} = -J \sum_{\langle (j,k)(m,n) \rangle} s_{j,k}\, s_{m,n}, \tag{3}$$

where $s_{j,k} = \pm 1$ is the spin value at x location j and y location k, and J is the coupling constant for interactions among the spins, and we set $J = 1$ during our simulations. The summation runs over all the nearest-neighbor spins, and $0 \leqslant (j,k,m,n) < L$. All properties we report here have been obtained by simulating the model at the critical temperature $T_c = 2/\ln(1+\sqrt{2})$ and by setting the value of the Boltzmann constant k_B to unity.

The model is simulated with Kawasaki dynamics at T_c. All simulations reported in this paper have been performed at zero (conserved) order parameter. In other words, we fix the total magnetization of the system at zero, and at each Monte Carlo move, two neighboring spins are randomly selected to exchange their values. The resulting energy change ΔE is measured, and the move is accepted with the normal Metropolis probability $\min[1, \exp(-\Delta E/T)]$. For each unit of time, on average, all the spins are supposed to be selected once.

B. Fourier modes for line magnetization

In this model we define the line magnetization as $M_l(j,t) = \sum_{k=0}^{L-1} s_{j,k}(t)$; correspondingly, the pth Fourier mode amplitude of the line magnetization is given by

$$A_p(t) = \frac{1}{L}\sum_{j=0}^{L-1} M_l(j,t)\exp(-2\pi i p j/L) = X_p(t) - iY_p(t), \tag{4}$$

where

$$X_p(t) = \frac{1}{L}\sum_{j=0}^{L-1} M_l(j,t)\cos(2\pi p j/L),$$
$$Y_p(t) = \frac{1}{L}\sum_{j=0}^{L-1} M_l(j,t)\sin(2\pi p j/L), \tag{5}$$

respectively, are the real and the imaginary parts of the Fourier transform, with $p = 0, 1, \ldots, (L-1)$. The inverse Fourier transform is then given by

$$M_l(j,t) = \sum_{p=0}^{L-1} A_p(t)\exp(2\pi i p j/L) \quad \text{or}$$
$$M_l(j,t) = \sum_{p=0}^{L-1} [X_p(t)\cos(2\pi p j/L) + Y_p(t)\sin(2\pi p j/L)]. \tag{6}$$

C. Equilibrium properties of the Fourier mode amplitudes

We express the equilibrium correlations of the Fourier modes as

$$X_{pq}(t) = \langle X_p(t) X_q(0)\rangle \quad \text{and} \quad Y_{pq}(t) = \langle Y_p(t) Y_q(0)\rangle, \tag{7}$$

where the angular brackets ($\langle\cdot\rangle$) define an average over equilibrated ensembles.

The cross-correlation terms, $\langle X_p(t)Y_q(0)\rangle$ and $\langle Y_p(t)X_q(0)\rangle$, respectively, can be argued to be equal to zero, as follows. Let us consider $\langle X_p(t)Y_q(0)\rangle$ to illustrate the calculation. First, having expressed it as $\sum_{j,m=0}^{L-1}\langle M_l(j,0)M_l(m,t)\rangle \cos(2\pi p j/L)\sin(2\pi q m/L)$, then making the simultaneous substitutions $j \to (L-j)$ and $m \to (L-m)$, and finally using $M_l(0,t) = M_l(L,t)$ due to periodic boundary conditions, we find that the term also equals $-\sum_{j,m=0}^{L-1}\langle M_l(L-j,0) M_l(L-m,t)\rangle \cos(2\pi p j/L)\sin(2\pi q m/L)$. Next, we use the fact that $\langle M_l(j,0)M_l(m,t)\rangle$ is only a function of $|j-m|$ modulo $L/2$ (due to periodic boundary conditions) as well as only of $|t|$ (due to time reversibility invariance at equilibrium). This implies that $\langle M_l(j,0)M_l(m,t)\rangle = \langle M_l(L-j,0)M_l(L-m,t)\rangle$, leading to the condition $\langle X_p(t)Y_q(0)\rangle = -\langle X_p(t)Y_q(0)\rangle = 0$. For this reason we leave both $\langle X_p(t)Y_q(0)\rangle$ and $\langle Y_p(t)X_q(0)\rangle$ out of further considerations.

Next, we argue that $X_{pp}(0) = Y_{pp}(0)$ at least up to $O(L^{-2})$. In order to do so, we first express $Y_{pp}(0)$ as $\sum_{j,m=0}^{L-1}\langle M_l(j,0)M_l(m,0)\rangle \sin(2\pi p j/L)\sin(2\pi p m/L) = \sum_{j,m=0}^{L-1}\langle M_l(j,0)M_l(m,0)\rangle, cos(2\pi p j'/L)\cos(2\pi p m'/L)$, where $(j',m') = (j+\frac{L}{4p}, m+\frac{L}{4p})$. We then again observe, just like above, that $\langle M_l(j,0)M_l(m,t)\rangle$ is only a function of $|j-m|$ modulo $L/2$. This implies that if $\frac{L}{4p}$ is an integer, then upon relabeling the line indices the sum trivially reduces to $\sum_{j',m'=0}^{L-1}\langle M_l(j',0)M_l(m',0)\rangle \cos(2\pi p j'/L)\cos(2\pi p m'/L) = X_{pp}(0)$. If, however, $\frac{L}{4p}$ is not an integer, then we can still relabel the indices as $\sum_{j'',m''=0}^{L-1}\langle M_l(j'',0)M_l(m'',0)\rangle \cos(2\pi p(j''+\Delta x)/L)\cos(2\pi p(m''+\Delta x)/L)$, with $\Delta x < 1$, 1 being the lattice unit. Beyond this point, we can do a Taylor expansion of the cosine terms, implying that the equality $Y_{pp}(0) = X_{pp}(0)$ must hold up to $O(L^{-2})$. This, together with the scaling of $\langle|A_p^2|\rangle \sim (L/p)^{\gamma/\nu}$ in the limit $p \to \infty$ for the 2D Ising model as derived in Appendix A, we attempt to fit $X_{pp}(0) = Y_{pp}(0)$ to the asymptotic scaling $\sim(L/p)^{\gamma/\nu}$ in Fig. 1.

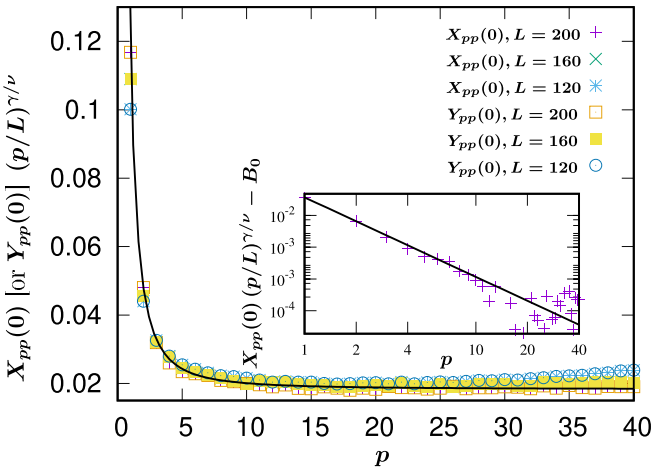

FIG. 1. $X_{pp}(0)$ and $Y_{pp}(0)$ as a function of p for different system sizes, with $p = 1$ to 40, and $L = 120$, 160, 200. Fitting to the data leads to $X_{pp}(0) = Y_{pp}(0) \approx (L/p)^{\gamma/\nu}\,(B_0 + B_1 p^{-\gamma/\nu})$, where $B_0 = 0.0185$ and $B_1 = 0.1$. Inset: $X_{pp}(0)$ data for $L = 200$ are fitted in a log-log plot; the straight line has slope $-1.75(= \gamma/\nu)$.

From this fit, we find that $X_{pp}(0) \approx Y_{pp}(0) \approx (L/p)^{\gamma/\nu}\,(B_0 + B_1 p^{-\gamma/\nu})$, where $B_0 = 0.0185$ and $B_1 = 0.1$ are two numerically obtained constants. Note also that

$$X_{p(L-q)}(t) = X_{pq}(t) \quad \text{and} \quad Y_{p(L-q)}(t) = Y_{pq}(t), \tag{8}$$

an obvious result obtained from the symmetry of the mode amplitudes under $p \leftrightarrow L - p$.

The results of Fig. 1 are supplemented with the data for $\chi_{pq}(0) \equiv X_{pq}(0)/\sqrt{X_{pp}(0)X_{qq}(0)}$ and $\Upsilon_{pq}(0) \equiv Y_{pq}(0)/\sqrt{Y_{pp}(0)Y_{qq}(0)}$ for $L = 40$ and $p, q < L/2$ (specifically, $p, q = 1$ to 10) in Fig. 2. The values of the off-diagonal elements of $\chi_{pq}(0)$ and $\Upsilon_{pq}(0)$ are not zero (we do not expect them to be zero even after caring for numerical accuracy); however, they are at least two orders of magnitude smaller than the diagonal ones.

Together these results indicate that to a very good approximation the modes remain statistically independent during the system's evolution by means of Kawasaki dynamics.

D. Fourier modes as approximate dynamical eigenmodes of the model

In Fig. 3(a) we obtain a data collapse plot for the mean-square deviation (MSD) of the complex mode amplitude $\langle|\Delta A_p^2(t)|\rangle$, as a function of $(p/L)^{z_c}t$ for $p = 1, 2, \ldots, 10$ for three different system sizes $L = 120$, 160, 200 (from our earlier works on spin systems [21–23] we expect that the data collapse would require scaling time with a prefactor $(p/L)^{z_c}$). The solid line in the figure then represents

$$\begin{aligned}\left\langle \Delta A_p^2(t)\right\rangle &= \sqrt{2}\left\langle \Delta X_p^2(t)\right\rangle = \sqrt{2}\left\langle \Delta Y_p^2(t)\right\rangle \\ &\approx 3.2527\left(\frac{L}{p}\right)^{\gamma/\nu}(p/L)^{z_c}t \quad \text{for} \quad (p/L)^{z_c}t \ll 1.\end{aligned} \tag{9}$$

Since the MSDs of the mode amplitudes can be expressed in terms of their autocorrelation functions as

$$\begin{aligned}\left\langle \Delta X_p^2(t)\right\rangle &= \langle [X_p(t) - X_p(0)]^2\rangle = 2X_{pp}(0)\left[1 - \frac{X_{pp}(t)}{X_{pp}(0)}\right], \\ \left\langle \Delta Y_p^2(t)\right\rangle &= \langle [Y_p(t) - Y_p(0)]^2\rangle = 2Y_{pp}(0)\left[1 - \frac{Y_{pp}(t)}{Y_{pp}(0)}\right],\end{aligned} \tag{10}$$

with the approximation $X_{pp}(0) = Y_{pp}(0) \approx (L/p)^{\gamma/\nu}\,(B_0 + B_1 p^{-\gamma/\nu})$, for $(p/L)^{z_c}t \ll 1$ in a large range shown in Fig. 3, Eqs. (9) and (10) can be recast in the form

$$\frac{X_{pp}(t)}{X_{pp}(0)} = \frac{Y_{pp}(t)}{Y_{pp}(0)} \approx \exp\left[-\frac{1.15(p/L)^{z_c}t}{0.0185 + 0.1\,p^{-\gamma/\nu}}\right]. \tag{11}$$

To conclude, in this section we have demonstrated that to a very good approximation the Fourier modes for the 2D Ising model with Kawasaki dynamics remain statistically uncorrelated at all times, and their autocorrelations decay exponentially in time, from which we conclude that they are approximate dynamical eigenmodes. This means that the properties of the modes' amplitude can be used to calculate all dynamical quantities to a very good approximation [1–3,12]. In the following section, we will showcase this to calculate the autocorrelation function and the MSD of line magnetizations.

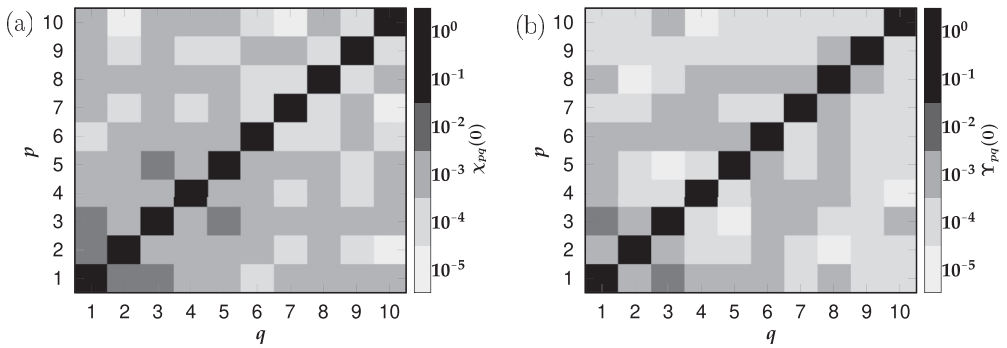

FIG. 2. The matrix (a) $\chi_{pq}(0) \equiv X_{pq}(0)/\sqrt{X_{pp}(0)X_{qq}(0)}$ and (b) $\Upsilon_{pq}(0) \equiv Y_{pq}(0)/\sqrt{Y_{pp}(0)Y_{qq}(0)}$ in logarithmic grayscale for $p, q = 1, 2, \ldots, 10$ and $L = 40$. The values of the off-diagonal elements of $\chi_{pq}(0)$ and $\Upsilon_{pq}(0)$ are not zero. However, most of them are typically two or more orders of magnitude smaller than the diagonal ones, which means the modes are statistically uncorrelated.

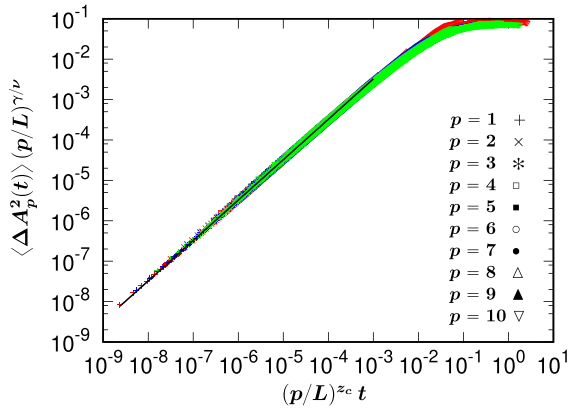

FIG. 3. The MSD of the complex modes amplitude $\langle |\Delta A_p^2(t)| \rangle = \sqrt{2}\,\langle \Delta Y_p^2(t) \rangle = \sqrt{2}\,\langle \Delta X_p^2(t) \rangle$, where $\langle \Delta X_p^2(t) \rangle = \langle [X_p(t) - X_p(0)]^2 \rangle$ and $\langle \Delta Y_p^2(t) \rangle = \langle [Y_p(t) - Y_p(0)]^2 \rangle$. For every system size $L = 120$ (red), 160 (blue), 200 (green), the MSD of 10 different mode amplitudes are measured. In the range $t \lesssim (p/L)^{z_c}$, the modes shows normal diffusion, and the solid line represents $\langle |\Delta A_p^2(t)| \rangle \, (p/L)^{\gamma/\nu} \approx 3.2527 \, (p/L)^{z_c} \, t$.

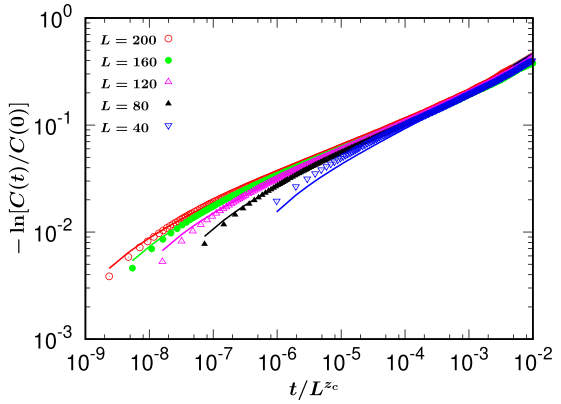

FIG. 4. Comparison between the simulation results (points) and expectation values from Eq. (13) (solid lines, same colors as the points) for the autocorrelation function $C(t)$ of the line magnetization, for different system sizes.

III. DYNAMICS OF TWO PHYSICAL OBSERVABLES USING THE FOURIER MODES AS APPROXIMATE DYNAMICAL EIGENMODES

In this section we focus on the dynamics observables of the system. Using the properties of the Fourier modes obtained in the last section, we analytically derive the autocorrelation function and the MSD of the line magnetization.

A. Autocorrelation function of the line magnetization

The first dynamical observable we are dealing with is the autocorrelation function of the line magnetization, defined as

$$C(t) = \langle M_l(x,t) M_l(x,0) \rangle. \tag{12}$$

This autocorrelation function can be expressed in terms of the modes by combining Eqs. (6), (8), and (12), yielding

$$\begin{aligned} C(t) &= 4 \sum_{p=1}^{L/2} X_{pp}(t) \\ &= 4 \sum_{p=1}^{L/2} \left(\frac{L}{p}\right)^{\gamma/\nu} \exp\left[-\frac{1.15\,(p/L)^{z_c} t}{0.0185 + 0.1\, p^{-\gamma/\nu}} \right] \\ &\quad \times (0.0185 + 0.1 p^{-\gamma/\nu}) \end{aligned} \tag{13}$$

As shown in Fig. 4, the prediction (13) fits the simulation results quite well.

B. Anomalous diffusion of the line magnetization

Let us now consider the MSD of the line magnetization

$$\left\langle \Delta M_l^2(t) \right\rangle = \langle [M_l(x,t) - M_l(x,0)]^2 \rangle \tag{14}$$

as another dynamical observable.

Using Eq. (6) and $\langle X_p(t) Y_q(0) \rangle = \langle Y_p(t) X_q(0) \rangle = 0$, we have

$$\begin{aligned} \left\langle \Delta M_l^2(t) \right\rangle = \sum_{p=0}^{L-1} \sum_{q=0}^{L-1} & \langle [X_p(t) - X_p(0)][X_q(t) - X_q(0)] \\ & \times \cos(2\pi px/L) \cos(2\pi qx/L) \\ & + [Y_p(t) - Y_p(0)][Y_q(t) - Y_q(0)] \\ & \times \sin(2\pi px/L) \sin(2\pi qx/L) \rangle. \end{aligned} \tag{15}$$

Then Eq. (15) can be simplified with the approximation $X_{pq}(t) = Y_{pq}(t) = X_{p(L-q)}(t) = Y_{p(L-q)}(t)$, and $X_0(t)$ as the conserved order parameter (chosen to be zero) of the dynamics, leading us to

$$\begin{aligned} \langle \Delta M_l^2(t) \rangle &= 2 \sum_{p=1}^{L-1} \sum_{q=1}^{L-1} [X_{pq}(0) - X_{pq}(t)] \\ &= 8 \sum_{p=1}^{L/2} \sum_{q=1}^{L/2} X_{pq}(0) \left[1 - \frac{X_{pq}(t)}{X_{pq}(0)} \right] \\ &= 8 \sum_{p=1}^{L/2} X_{pp}(0) \left[1 - \frac{X_{pp}(t)}{X_{pp}(0)} \right]. \end{aligned} \tag{16}$$

Using the properties of $X_{pp}(t)$ and $X_{pp}(0)$ as obtained in Secs. II C and II D, the behavior of the MSD of the line magnetization can be divided into two time domains.

At long times $t \gtrsim L^{z_c}$, $\frac{X_{pp}(t)}{X_{pp}(0)} \to 0$, meaning that $\langle \Delta M_l^2(t) \rangle$ approaches a constant $\sim L^{\gamma/\nu}$. At intermediate times $1 \lesssim t \lesssim L^{z_c}$,

$$\left\langle \Delta M_l^2(t) \right\rangle = 8 \sum_{p=1}^{L/2} X_{pp}(0) \left[1 - \frac{X_{pp}(t)}{X_{pp}(0)} \right] = 8 \sum_{p=1}^{L/2} \left(\frac{L}{p}\right)^{\gamma/\nu} \left\{ 1 - \exp\left[-\frac{1.15\,(p/L)^{z_c} t}{0.0185 + 0.1\, p^{-\gamma/\nu}} \right] \right\} (0.0185 + 0.1 p^{-\gamma/\nu}). \tag{17}$$

As shown in Fig. 5(a), the prediction (17) fits the simulation results quite well.

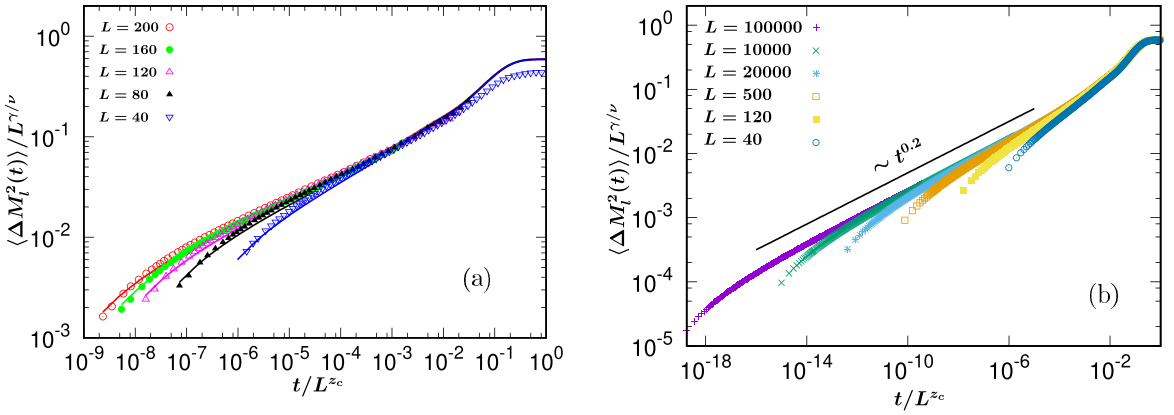

FIG. 5. (a) Comparison between the simulation results (points) and the results obtained from Eq. (17) (solid lines, same color as the points) for the MSD of the line magnetization $\langle \Delta M_l^2(t) \rangle$ for different system sizes. (b) Confirmation of the sum (19) to power law $t^{(\gamma/\nu-1)/z_c} \approx t^{0.2}$ for $L \to \infty$.

For an analytical expression for the MSD, with $x = p/L$, the sum (17) can be reduced to the following integral:

$$\langle \Delta M_l^2(t) \rangle = 8L \int_{1/L}^{1/2} \frac{dx}{x^{\gamma/\nu}} \left(1 - \exp\left\{ - \frac{1.15\, t x^{z_c}}{[0.0185 + 0.1/(xL)^{\gamma/\nu}]} \right\}\right) [0.0185 + 0.1/(xL)^{\gamma/\nu}], \tag{18}$$

but beyond that it is difficult process it further without making approximations. In particular, in the limit $L \to \infty$ and finite values of x, the second term within the curly brackets can be dropped. At the lower limit of x, the two terms within the curly brackets are, however, comparable. Nevertheless, if we do drop this second term altogether, then the integral can be easily performed to show that in the leading order of L

$$\begin{aligned} \langle \Delta M_l^2(t) \rangle &\sim L \left(\frac{t}{L} \right)^{(\gamma/\nu - 1)/z_c} \\ &\Rightarrow \langle \Delta M_l^2(t) \rangle \sim L^{\gamma/\nu} \left(\frac{t}{L^{z_c}} \right)^{(\gamma/\nu - 1)/z_c} \\ &\approx L^{\gamma/\nu} \left(\frac{t}{L^{z_c}} \right)^{0.2}. \end{aligned} \tag{19}$$

This behavior of the sum (19) is shown in Fig. 5(b).

IV. GENERALIZED LANGEVIN EQUATION FORMULATION FOR THE ANOMALOUS DIFFUSION IN THE ISING MODEL WITH KAWASAKI DYNAMICS

In Sec. III we have demonstrated that at the intermediate time regime, the line magnetization in the Ising model with Kawasaki dynamics exhibits anomalous diffusion. In our recent studies on the Ising and ϕ^4 model with Glauber dynamics [22,23], we have argued that the anomalous diffusion of the magnetization belongs to the GLE class, for which the restoring force plays an important role.

Imagine that we choose a tagged line, and since the thermal spin flips, at $t = 0$ its magnetization M_l changes by a little amount δM_l. The surrounding spins will react to this change due to the interactions dictated by the Hamiltonian, and it takes time to spread this reaction. During this time, the value of M_l will also readjust to the persisting values of the surrounding spins, undoing at least a part of δM_l. It is the latter that we interpret as the result of "inertia" of the surrounding spins that resists changes in M_l, and the resistance itself acts as the restoring force to the changes in the tagged magnetization, and finally, leads to anomalous diffusion.

A. Generalized Langevin equation for the line magnetization

From how the restoring force works introduced before, it not only indicates that there is a memory effect which is significant during the "restoring" process, but also leads us to the GLE formulation to describe the anomalous diffusion.

In line with our previous works on the Ising and ϕ^4 model with Glauber dynamics [22,23] and in polymeric systems [3,24–26], the relation of the restoring force $f(t)$ and the "velocity" of magnetization $\dot{M}_l(t)$ can be expressed as

$$\zeta \dot{M}_l(t) = f(t) + q_1(t) \tag{20a}$$

$$f(t) = -\int_0^t dt' \mu(t - t') \dot{M}_l(t') + q_2(t). \tag{20b}$$

Here $f(t)$ is the internal force, ζ is the "viscous drag" on M_l, $\mu(t - t')$ is the memory kernel, $q_1(t)$ and $q_2(t)$ are two noise terms satisfying $\langle q_1(t) \rangle = \langle q_2(t) \rangle = 0$, and the fluctuation-dissipation theorems (FDTs) are given by $\langle q_1(t)\, q_1(t') \rangle \propto \zeta \delta(t - t')$ and $\langle q_2(t)\, q_2(t') \rangle \propto \mu(t - t')$ respectively.

Equation (20b) can be inverted to write as

$$\dot{M}_l(t) = -\int_0^t dt'\, a(t - t') f(t') + \omega(t). \tag{21}$$

The noise term $\omega(t)$ similarly satisfies $\langle \omega(t) \rangle = 0$, and the FDT $\langle \omega(t) \omega(t') \rangle = a(|t - t'|)$. Then $a(t)$ and $\mu(t)$ are related to each other in the Laplace space as $\tilde{a}(s)\tilde{\mu}(s) = 1$.

To combine Eqs. (20a) and (20b), we obtain

$$\zeta \dot{M}_l(t) = -\int_0^t dt' \mu(t-t') \dot{M}_l(t') + q_1(t) + q_2(t) \quad (22)$$

or

$$\dot{M}_l(t) = -\int_0^t dt' \theta(t-t') [q_1(t) + q_2(t)], \quad (23)$$

where in the Laplace space $\tilde{\theta}(s)[\zeta + \tilde{\mu}(s)] = 1$. With $t > t'$, without any loss of generality, using Eq. (23) the result of the velocity autocorrelation is

$$\langle \dot{M}_l(t) \dot{M}_l(0) \rangle \sim \theta(t-t'), \quad (24)$$

where $\theta(t)$ can be calculated by Laplace inverting the relation $\tilde{\theta}(s)[\zeta + \tilde{\mu}(s)] = 1$.

If the memory term is a power law in time,

$$\mu(t) \sim t^{-c}. \quad (25)$$

Using the results from Ref. [25], we have

$$\langle \dot{M}_l(t) \dot{M}_l(0) \rangle|_{f=0} \sim -(t-t')^{c-2}. \quad (26)$$

By integrating Eq. (26) twice in time, we obtain that

$$\left\langle \Delta M_l^2(t) \right\rangle \sim t^c. \quad (27)$$

In summary, there is a power-law memory function $\mu(t) \sim t^{-c}$ which plays a vital part in the GLE formulation. From this we can deduce that the anomalous diffusion found in Eq. (17) is non-Markovian and the anomalous exponent is c.

B. Verification of the power-law behavior of $\mu(t)$

Based on the FDT mentioned under Eq. (20b), we now numerically verify the behavior of $\mu(t)$.

During simulations, at $t = 0$, we thermalize the system to its equilibrium state. For $t > 0$ we select a line and fix its value of the magnetization M_l by performing nonlocal spin-exchange dynamics, i.e., we choose two lattice sites (j,k) and (m,n), and if $s_{j,k}s_{m,n} = -1$ then we exchange their values, otherwise we keep their values as they are. The energy change ΔE is measured, and we accept the move with the Metropolis probability $\min[1, \exp(-\Delta E/T)]$. For the rest of the system, we let them evolve with the Kawasaki dynamics.

We then keep taking snapshots of the system at regular intervals. For every snapshot we take, we consider an attempt to flip each spin in turn and find the expected change in M_l which would have occurred if this move had been implemented, totaled over all the spins on the selected line, and the possible change of the line magnetization is defined as $f(t) = \dot{M}(t)$. The quantity $\langle f(t)f(0) \rangle$ is plotted in Fig. 6. The figure is in good agreement with our expectation that $\mu(t) \sim t^{-(\gamma/\nu-1)/z_c}$; this result has also been observed for the the 2D Ising model with Glauber dynamics [22].

V. CONCLUSION

In this paper, we have studied the Fourier modes of the 2D Ising model with Kawasaki dynamics at critical temperature and at zero (conserved) order parameter. We have established that the Fourier modes are the dynamical eigenmodes of the system to a very good approximation. Using these modes, we can reconstruct the dynamics of any dynamical variable; we have done so for the autocorrelation function and the mean-square deviation (MSD) of line magnetization.

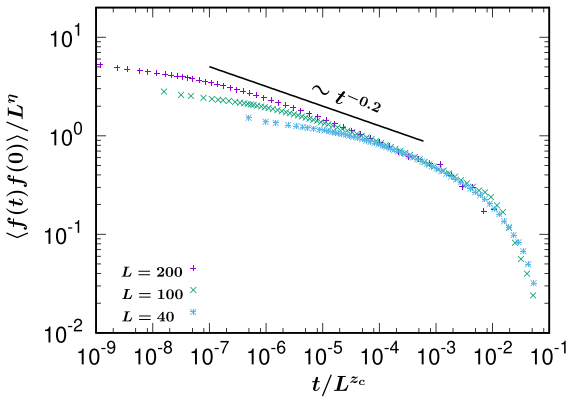

FIG. 6. The autocorrelation function $\langle f(t)f(0)\rangle$ as a function of time; the solid line corresponds to $\langle f(t)f(0)\rangle \sim t^{-(\gamma/\nu-1)/z_c} \approx t^{-0.2}$.

At the intermediate times, we have found that for $1 \lesssim t \lesssim L^{z_c}$, the line magnetization undergoes anomalous diffusion. We have argued that like other spin models and polymeric systems this anomalous behavior can be described by the GLE formulation with a memory kernel. The corresponding fluctuation-dissipation theorem has been verified by the calculation of the force autocorrelation.

With these results, we have showcased that for Kawasaki dynamics, the Fourier modes, as the approximate dynamical eigenmodes, are a useful tool to analytically derive the dynamical quantities in the Ising system. We note, however, that if the model is evolved using Glauber dynamics, then we find that $X_{pp}(t)$ decays as a stretched exponential in time (not shown in this paper), which clearly shows that the Fourier modes are not the (approximate) dynamical eigenmodes. We

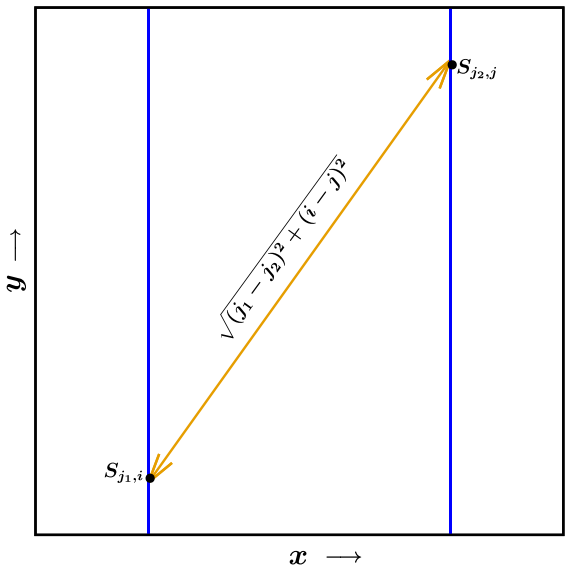

FIG. 7. Schematic diagram for the calculation of the line-line autocorrelation function.

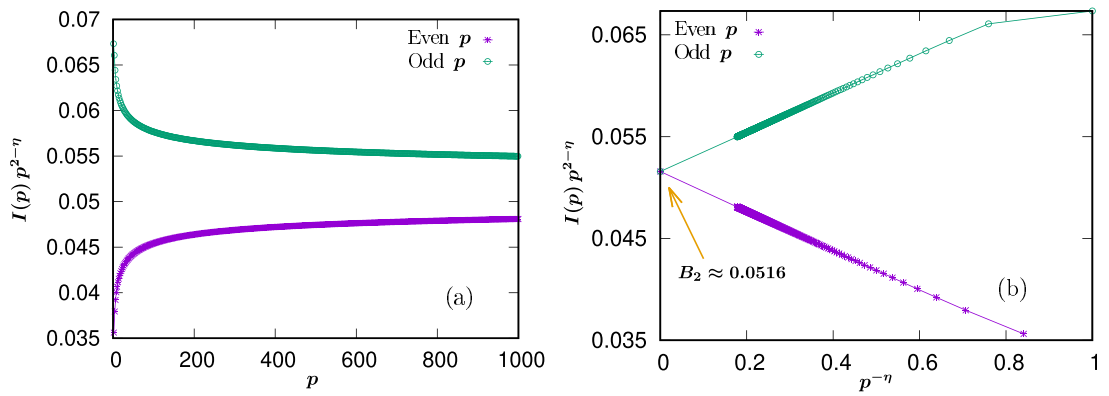

FIG. 8. (a) Numerical integration of the integral in Eq. (A6). (b) $I(p) \approx B_2\, p^{2-\eta}$ in the limit $p \to \infty$, where $B_2 \approx 0.0516$, although convergence to the asymptotic behavior is rather slow. The solid lines are fits to the data.

do not understand this at present. It could be explored in the future.

ACKNOWLEDGMENTS

We thank R. C. Ball for valuable discussions. W.Z. acknowledges financial support from the China Scholarship Council (CSC).

APPENDIX: SCALING OF $\langle|A_p|\rangle^2$ WITH p FOR THE 2D ISING MODEL

In this Appendix we obtain the scaling behavior of $\langle|A_p|^2\rangle$ for the 2D Ising model (note that the calculations presented here do not correspond to the total magnetization of the sample kept fixed at zero, as is the case for Kawasaki dynamics in this paper).

First, we calculate the autocorrelation function of the line magnetization. We use the classic result that at the critical temperature the spin-spin autocorrelation function decays as $r^{-\eta}$, where r is the Euclidean distance between the two spins and $\eta = 2 - \gamma/\nu = 0.25$ for the 2D Ising model. With that knowledge, upon summing over i and j in the y direction (see Fig. 7), we obtain

$$\langle M_l(j_1,0)M_l(j_2,0)\rangle = \sum_{i=0}^{L-1}\sum_{j=0}^{L-1}\langle s_{j_1,i}\, s_{j_2,j}\rangle \sim \sum_{i=0}^{L-1}\sum_{j=0}^{L-1}[(i-j)^2+(j_2-j_1)^2]^{-\eta/2}. \tag{A1}$$

We next set $a = (j_1 - j_2)/L$, $u = (i-j)/L$ and $v = j/L$ to write

$$\langle M_l(j_1,0)M_l(j_2,0)\rangle \sim \int_{-1}^{1} du\, \frac{L^{2-\eta}}{[u^2+4a^2]^{\eta/2}}. \tag{A2}$$

The calculation of $\langle|A_p|^2\rangle$ follows from Eq. (A2) in a similar manner:

$$\langle|A_p|^2\rangle = \frac{1}{L^2}\sum_{j_1=0}^{L}\sum_{j_2=0}^{L}\langle M_l(j_1,0)M_l(j_2,0)\rangle \times \cos[2\pi p(j_1-j_2)/L]. \tag{A3}$$

This time setting $a \to a/2$, Eq. (A3) reduces to

$$\langle|A_p|^2\rangle \sim L^{2-\eta}\int_{-1}^{1} da \int_{-1}^{1} du\, \frac{1}{[u^2+a^2]^{\eta/2}}\cos(\pi pa) = 4L^{2-\eta}\int_{0}^{1} da \int_{0}^{1} du\, \frac{1}{[u^2+a^2]^{\eta/2}}\cos(\pi pa). \tag{A4}$$

For $p = 0$, Eq. (A4) leads to $|A_p(0)|^2 \sim L^{2-\eta}$, which is the classic result for the equilibrium scaling $\langle M^2\rangle \sim L^{4-\eta} = L^{2+\gamma/\nu}$ for the total sample magnetization M for the 2D Ising model.

For $p \neq 0$ we perform the integration over u in Eq. (A4) to obtain

$$\langle|A_p|^2\rangle \sim L^{2-\eta}\underbrace{\int_0^1 da\, f(a)\cos(\pi pa)}_{I(p)}, \tag{A5}$$

with

$$f(a) = \frac{(1+a^2)^{1-\eta/2}(5+a^2-\eta)}{(4-\eta)(2-\eta)} - \frac{(1+a^2)^{3-\eta/2}\ \text{Hypergeometric}_2F_1[1,(3-\eta)/2,-1/2,-1/a^2]}{a^2(4-\eta)(2-\eta)}. \tag{A6}$$

We then perform numerical integration separately for even and odd p values for Eq. (A6). The results, shown in Fig. 8, demonstrate that in the limit $p \to \infty$

$$\langle|A_p|\rangle^2 \sim \left(\frac{L}{p}\right)^{2-\eta} = \left(\frac{L}{p}\right)^{\gamma/\nu}, \tag{A7}$$

although convergence to the asymptotic behavior is rather slow.

[1] M. Doi, *Introduction to Polymer Physics* (Oxford University Press, Oxford, 1996).

[2] M. Doi and S. F. Edwards, *The Theory of Polymer Dynamics* (Clarendon Press, Oxford, 1988).

[3] R. Keesman, G. T. Barkema, and D. Panja, J. Stat. Mech. (2013) P02021.

[4] D. Nelson, T. Piran, and S. Weinberg, *Statistical Mechanics of Membranes and Surfaces* (World Scientific, Singapore, 2004).

[5] R. Keesman, G. T. Barkema, and D. Panja, J. Stat. Mech. (2013) P04009.

[6] R. Lipowsky and E. Sackmann, *Structure and Dymanics of Membranes, Handbook of Biological Physics* (Elsevier Science, Amsterdam, 1995), Vol. 1.

[7] C. Picart and D. E. Discher, Biophys. J. **77**, 865 (1999).

[8] E. Sackmann, ChemPhysChem **3**, 237 (2002).

[9] T. Hwa, E. Kokufuta, and T. Tanaka, Phys. Rev. A **44**, R2235(R) (1991).

[10] M. S. Spector, E. Naranjo, S. Chiruvolu, and J. A. Zasadzinski, Phys. Rev. Lett. **73**, 2867 (1994).

[11] X. Wen *et al.*, Nature (London) **355**, 426 (1992).

[12] D. Panja and G. T. Barkema, J. Chem. Phys. **131**, 154903 (2009).

[13] G. T. Barkema, D. Panja, and J. M. J. van Leeuwen, J. Chem. Phys. **134**, 154901 (2011).

[14] T. Kreer, J. Baschnagel, M. Muller, and K. Binder, Macromolecules **34**, 1105 (2001).

[15] J. T. Kalathi, S. K. Kumar, M. Rubinstein, and G. S. Grest, Soft Matter **11**, 4123 (2015).

[16] J. T. Kalathi, S. K. Kumar, M. Rubinstein, and G. S. Grest, Macromolecules **47**, 6925 (2014).

[17] K. Kawasaki, Phys. Rev **145**, 224 (1966).

[18] B. I. Halperin, P. C. Hohenberg, and S. K. Ma, Phys. Rev. B **10**, 139 (1974).

[19] M. C. Yalabik and J. D. Gunton, Phys. Rev. B **25**, 534(R) (1982).

[20] F. J. Alexander, D. A. Huse, and S. A. Janowsky, Phys. Rev. B **50**, 663 (1994).

[21] J.-C. Walter and G. T. Barkema, Physica A **418**, 78 (2015).

[22] W. Zhong, D. Panja, G. T. Barkema, and R. C. Ball, Phys. Rev. E **98**, 012124 (2018).

[23] W. Zhong, G. T. Barkema, D. Panja, and R. C. Ball, Phys. Rev. E **98**, 062128 (2018).

[24] D. Panja, J. Stat. Mech. (2010) L02001.

[25] D. Panja, J. Stat. Mech. (2010) P06011.

[26] D. Panja, J. Phys.: Condens. Matter **23**, 105103 (2011).

[27] C. Maes and S. R. Thomas, Phys. Rev. E **87**, 022145 (2013).

[28] J. T. Bullerjahn, S. Sturm, L. Wolff, and K. Kroy, Europhys. Lett. **96**, 48005 (2011).

[29] H. Popova and A. Milchev, Phys. Rev. E **77**, 041906 (2008).

[30] K. Mizuochi, H. Nakanishi, and T. Sakaue, Europhys. Lett. **107**, 38003 (2014).

[31] D. Panja, G. T. Barkema, and R. C. Ball, J. Phys.: Condens. Mattter **19**, 432202 (2007).

[32] D. Panja, G. T. Barkema, and R. C. Ball, J. Phys.: Condens. Matter **20**, 075101 (2008).

[33] D. Panja and G. T. Barkema, Biophys. J. **94**, 1630 (2008).

[34] J. L. A. Dubbeldam, V. G. Rostiashvili, A. Milchev, and T. A. Vilgis, Phys. Rev. E **83**, 011802 (2011).

[35] H. Vocks, D. Panja, G. T. Barkema, and R. C. Ball, J. Phys.: Condens. Matter **20**, 095224 (2008).

[36] D. Panja, G. T. Barkema, and A. B. Kolomeisky, J. Phys.: Condens. Matter **21**, 242101 (2009).

[37] T. Saito and T. Sakaue, Phys. Rev. E **92**, 012601 (2015).